

# GPS Ocean Surface Reflection Technology Requirements for Space Applications

Task: GOALS Requirements (GOALS: GPS-Based Oceanographic and Atmospheric Low-Earth  
Orbiting Sensor)

Trade Study Area: Novel GPS Options

Cinzia Zuffada (Cinzia.Zuffada@jpl.nasa.gov)  
George Hajj (George.Hajj@jpl.nasa.gov)  
Steve Lichten (Stephen.M.Lichten@jpl.nasa.gov)

**Final Report**

**October 21, 1998**

## **1. Introduction and motivation**

Two key NASA OES research objectives are the Seasonal to Interannual Climate Variability and Prediction and Long-Term Climate/Natural Variability and Change investigations. Altimetry missions are used to monitor sea height and can be used to monitor global events such as the El Nino, as has been done with Topex/Poseidon. While these measurements tie in closely with a third OES objective — Natural Hazards Research — to understand global climate change, it is essential to know how much heat the oceans and atmosphere are carrying. Estimates can be inferred from precision radar altimetry. Ocean eddies play an important role in current dynamics and in the global heat transport. Significant ocean energy is concentrated at a small physical length scale known as the radius of deformation, which varies from about 100 km near the equator to about 10 km at higher latitudes. Eddies are like the “storms” of the ocean, and extract energy from the upper (wind driven) layers of circulation and transfer it to greater depth. Existing ocean models, including those used in the important climate forecasting coupled ocean-atmosphere models, are far from properly resolving ocean eddies, and therefore the uncertainties associated with the model output remain undetermined. Because eddies are typically only a few hundred km across and have relatively short lifetimes, the 10 day repeat cycle and 300 km crosstrack spacing of TOPEX/POSEIDON and JASON make it impossible to observe and track each eddy that may occur. The new remote sensing instrument (GOALS) we are investigating in this study effort provides the technology to enable monitoring of ocean eddies through ocean reflections of Global Positioning System (GPS) signals. We estimate that global sub-decimeter ocean height accuracy in 4 days over 25-50 km scales could be achieved for a constellation of low-Earth orbiters with GOALS (GPS) receivers tracking all the Global Navigation Satellite System (GNSS = GPS + GLONASS) signals, suitable for ocean mesoscale flow or eddy studies of heat transport. Associated ocean height anomalies of 50 cm typically drift ~ 5-10 km/day, so this will enable observation of eddy formation and evolution and allow eddies to be tracked precisely between JASON samples. We also note here the potential for commercial exploitation of this technology. The improved knowledge of the ocean surface conditions, available globally and rapidly with this remote sensing instrument, could dramatically impact shipping operations and choice of routing for commercial and military vessels. Efficiency improvements in such operations have the potential for very large cost savings.

## 2. Instrument description and challenges

### 2.1 Remote sensing of the sea

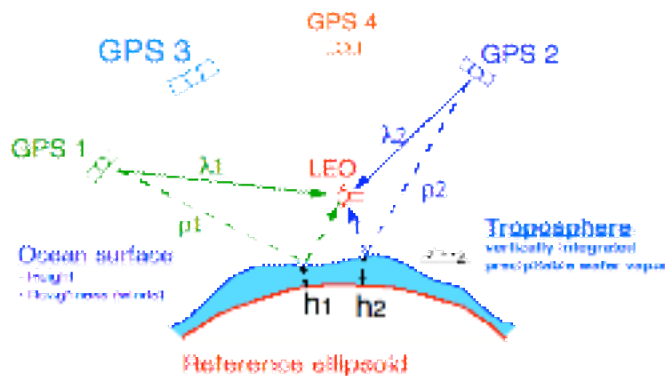


Fig. 2.1 GPS Bistatic Altimeter

The dashed lines in Fig. 2.1 depict the new measurements which are incorporated in this system, ocean surface reflected GPS signals simultaneously tracked and processed in the flight receiver. The reflected GPS signals from the ocean must be successfully detected and compared precisely with the direct GPS signals in order to infer the characteristics of the ocean from the combined data set. To accomplish this a preliminary theoretical assessment of the expected signal level and characteristics must be performed, in order to understand the necessary requirements of a space-based receiver to make these measurements. Furthermore, understanding the received signal structure is necessary in

order to extract from it the quantities describing sea state, such as sea height, roughness and wind speed. Ultimately, the usefulness of this instrument rests with the accuracy with which such parameters can be estimated. There are many challenges in developing a GPS receiver which has the capability and sensitivity to make these measurements. We intend to address these challenges in the present task in order to obtain design requirements for a space-based instrument.

### 2.2 Complementary capabilities

In the last decade the GPS constellation of 24 L-band satellites in 12-hr Earth orbits has transformed Earth remote sensing. From space-based platforms supported by GPS precision tracking, broad and encompassing scientific observables and measurements are available, providing unprecedented insight into oceanic and climatological processes and global change. Examples of this include precise orbit determination (POD) for ocean altimetric satellites, and Earth-limb occultation measurements of the atmosphere from low-Earth orbiters (LEOs). Significant results have been obtained from Topex/Poseidon and from GPS/MET [Bertiger et al. 1994; Kursinski et al. 1996; Kursinski and Hajj, 1998]. A recent enhancement to the JPL GPS analysis system has reduced position solution latency to less than 1 hr. POD techniques are also utilized in occultation analysis, since the position, and more importantly, the velocity of the LEO must be precisely known. When a radio signal is occulted by the atmosphere, its phase and amplitude are perturbed in a manner related to the vertical refractivity profile. Phase perturbations give direct information on refractivity, from which we can determine density, pressure, and temperature. GPS/MET data analysis [Kursinski et al., 1996, Ware et al., 1996] demonstrated that GPS/MET derived temperatures are accurate to better than 2 K in the altitude range 5-30 km when compared to analysis from the European Center for Medium-range Weather Forecast (ECMWF). Comparisons with ECMWF analysis also indicates that GPS/MET derived pressure geopotential heights are accurate to better than 20 gpm, [Leroy, 1997] between 5- 30 km, and that water vapor (derived by assuming knowledge of temperature) is accurate to 200 ppm in the middle and lower troposphere [Kursinski and Hajj, 1998]. Hence, GPS observables from low-Earth orbiters obtained from up-looking and limb-sounding antennas could be combined with a new, rich set of measurements derived from tracking GPS signals reflected off the ocean surface with a special nadir-looking antenna to form a multifunctional all-weather instrument.

## 3. Task Objectives

Because of the relative newness of the GOALS technique, we will provide a brief outline of the concept to provide the framework for the specific task objectives. The instrument operates in a

bistatic geometry (i.e., the transmitted and received signals travel two different paths) with the following distinctive features:

(1) Traditional altimetry is limited to looking in the nadir direction and obtaining one height observation at a time below the altimeter; by contrast, up to 20 ocean height measurements are possible simultaneously by tracking all reflected GNSS signals with a single receiver. One

such receiver in LEO will provide nearly 1.4 million 1-sec measurements of ocean heights per day.

(2) In traditional altimetry/scatterometry the coverage is regular according to a certain repeat pattern. Additionally, each measurement in itself provides an accurate estimate of the sea state parameters of interest. By contrast, GNSS reflection coverage is very dense but random. With the modest signal-to-noise ratios obtainable with a realistic antenna, single shot measurements do not in themselves provide an accurate estimate of all the sea state parameters of interest. Therefore spatial and temporal averaging of many measurements is required. Since the receiving satellite tracks do not repeat exactly, measurements points distributed in a given area will be used to refine the local solution as a function of time, and will define the spatial resolution.

In order to make this instrument viable in space we need to detect and process many scattered signals. Hence we need to understand what configurations of antenna gain and orientations capture the largest number of viable signals to be used in the subsequent spatial/temporal averaging process. The first objective of the present task is determining the best trade-offs between gain, sky coverage, coherence time and resolution.

The second objective is a more detailed signal analysis performed as a function of the instrument parameters and the sea state, such as roughness, expressed as wind speed amplitude. This second phase allows us to predict signal waveforms as a function of the sea state and for the antenna systems and configurations of interest. Some of the basic issues regarding the necessary correlator channels and receiver bandwidths can be understood from this work and used in the hardware design.

#### **4. Determining receiver antenna gain and pointing direction**

##### **4.1 Summary of findings**

Sensing GPS signals reflected off the ocean's surface from low-Earth orbit (LEO) for altimetry or scatterometry applications is meant to be a cheap and powerful approach of obtaining ocean height and roughness with very dense and rapid coverage. Essential to the success of these new GPS applications is the ability to see multiple GPS reflected signals simultaneously. This requires an antenna with a wide field-of-view pointing toward the Earth. In addition, since the reflected signal is generally weak, the receiving antenna needs to have a very high gain in order to achieve a reasonable accuracy. The combination of both of these requirements, namely high gain and wide field-of-view, could be satisfied with a large steerable antenna array, but this approach might prove to be expensive, making the GPS signal reflection application not an attractive technology.

In our study an alternative is suggested to the prevailing assumption that it is best to point the antenna in the nadir direction. It is argued that the closer to the limb we can point, the narrower the antenna beam width and the less gain we would need for the GPS ocean reflection to work. This is primarily because of the following two factors:

1) The effective solid area defined by the reflected signals for a given receiving antenna beamwidth (Fig. 4.1) gets larger for larger incident angles, causing the number of visible GPS reflected signals to get larger. For instance, an antenna with a 14° half-power beamwidth (HPBW) and a full azimuthal coverage will see ~9 GPS reflected signals when pointing close to the limb. By contrast, seeing the same number of satellites by pointing toward nadir requires an antenna HPBW of ~120° (i.e., ±60° from nadir) and full azimuthal coverage.

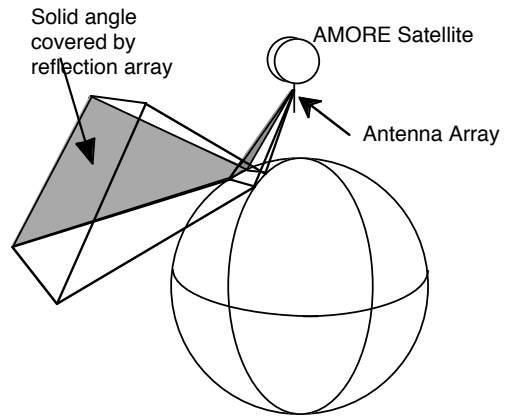


Fig. 4.1: A pictorial view of bistatic ocean reflection and the solid angle covered by an antenna in low-Earth orbit

2) The signal-to-noise ratio (SNR) of the reflected signal when arriving at the receiver is higher for low-elevation reflections (elevation here is defined as the angle between the reflected signal and the local tangent plane). For instance, for a 20 dBi antenna gain, voltage signal-to-noise ratio and range accuracy will improve by a factor of 2 for reflections at 15° elevation relative to reflections at 90° elevation. This is equivalent to having an additional 6 dB of gain. Substantially more SNR and better accuracy is obtained for elevations less than 15°. (See Fig. 4.2 for a summary).

This is equivalent to having an additional 6 dB of gain. Substantially more SNR and better accuracy is obtained for elevations less than 15°. (See Fig. 4.2 for a summary).

### 4.3 Signal-to-noise ratio analysis

The power signal-to-noise ratio (PSNR) for the reflected signal is given by the radar equation

$$PSNR = \frac{P_t G_t \sigma A}{4D^2 4d^2} \frac{G_r}{4} \frac{1}{kTB} \quad (1)$$

with  $P_t$  transmitted power,  $G_t$  transmitter's antenna gain,  $d$  and  $D$  are distances between reflection point and receiver and transmitter, respectively,  $\sigma$  surface scattering cross section per unit area,  $A$  reflective area on the ocean set by the Doppler and range filters of the receiver,  $\lambda$  GPS carrier wavelength,  $G_r$  receiver's antenna gain,  $k$  Boltzmann's constant,  $T$  system temperature,  $B$  Doppler bandwidth in the receiver (the inverse of the coherent integration time).

We note that  $D$ ,  $d$ ,  $A$  and  $B$  are all elevation dependent. The scattering cross section  $\sigma$  is also elevation dependent; however, in order to avoid the complications of studying the interaction of the electromagnetic waves with a rough surface, we take  $\sigma$  to be constant in this study.

Based on these assumptions, we first estimate VSNR for a single coherent measurement (i.e., before incoherent averaging). By incoherently averaging VSNR over four seconds we obtain the VSNR and corresponding range accuracy (given by P-code chip/VSNR) shown Figs. 4.2. In obtaining these VSNR the P-code is assumed to be known (no encryption); in the presence of anti-spoofing (AS), the same results can be obtained by assuming an additional 3 dB of gain for the reflection antenna and about 10 dB of gain for the antenna receiving the direction signal<sup>1</sup>.

<sup>1</sup> Brooks Thomas 1998 personal communication

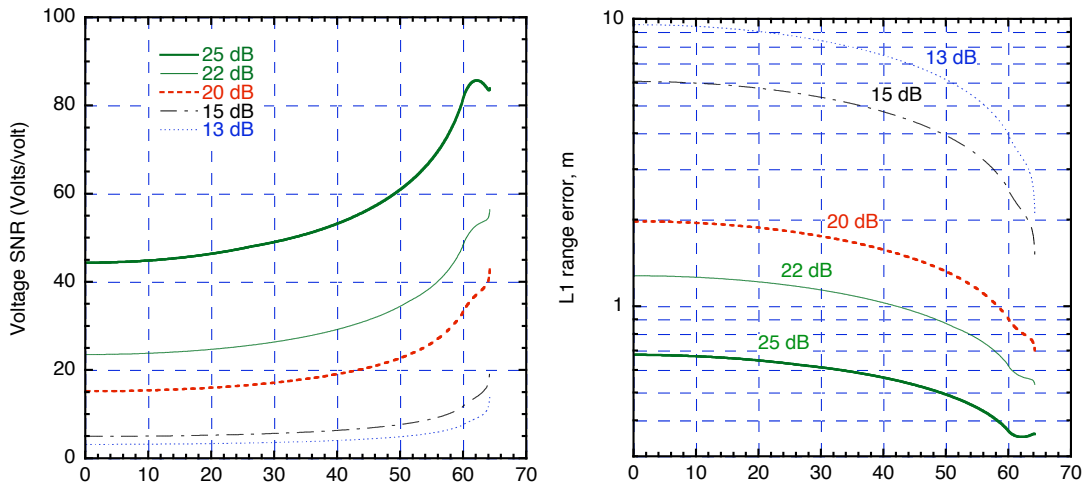


Fig. 4.2: Voltage signal-to-noise ratio (left) and corresponding  $L1$  range errors (right) after 4 second of incoherent averaging. A Doppler filter is used to maintain a maximum footprint size of 50 km (in the incident plane). In the presence of encryption, the same results can be obtained by assuming an additional 3 dB of gain for the reflection antenna and about 10 dB of gain for the antenna receiving the direct signal.

We note that the improvement in VSNR at low-elevation vs. high elevation is better for lower antenna gains. This is due to the fact that low VSNR ( $< \sim 1$ ) scale differently than large VSNR [Lowe, 1998]. In the limit of very large gains, the SNR curve becomes nearly flat because the increase in coherence time at low elevations is compensated for by incoherently averaging over fewer samples.

The improved accuracy seen in Fig. 4.2 is appreciable. For instance, based on the figure, a 20 dB antenna gives as 2 m range accuracy at normal incidence and 0.9 m range accuracy at  $\theta = 60^\circ$  ( $\theta = 16^\circ$ ). This is equivalent to having more than additional 6 dB of gain. The gain is even more substantial at lower elevations.

#### 4.6 Possible problematic issues for further investigation

*Atmospheric effects* : At low-grazing-angles one would have to worry about magnified errors introduced by propagation in the intervening media—the ionosphere and the troposphere. With a dual frequency system the ionosphere should be solvable. The increased sensitivity to the neutral atmosphere is advantageous for separating the ocean height and the atmosphere based on their mapping function. In fact, *at grazing incidence, the very high SNR and low sensitivity to ocean height suggest that ocean reflection will serve as an extremely powerful technique for atmospheric sensing*. These type of measurements, if thought of as an extension to the occultation measurements, will more than double the occultation coverage. Zuffada et al, [1998] have demonstrated that range measurements collected at very low-elevations can be used to obtain profiles of refractivity in the lower troposphere. Further research is needed to fully assess the benefits of ocean reflection for atmospheric sensing.

*Large footprints*: In order to circumvent the resolution limit set by the elongated elliptical footprints at grazing incidence, one can, in principle, combine overlapping footprints obtained from different LEO/GPS pairs to extract features that are smaller than the footprint. This can be done through tomographic techniques where an image is constructed from projections; in our case, each projection corresponds to a large footprint.

*Shadowing*: A careful examination is needed to account for shadowing effects, namely the obstruction of the electromagnetic wave as it reflects by large ocean waves.

## **5. Modeling the Expected Received Signal**

### **5.1 Basic issues**

When the GPS signal impinges on the ocean surface, the signal is scattered in all directions with maximum power in the direction of specular reflection. By measuring the time of arrival and the level of power return in the specular direction we can detect the mean surface height, mean surface slope, wind speed amplitude and significant wave heights near the specular point. Because the ocean reflectance depends on the surface temperature and salinity, measuring the return power with sufficient accuracy can, in principle, be used to infer these physically important parameters. A quantitative estimate of the received signal is given by the radar equation.

The main objective of this study is to understand and model the basic signal processing mechanisms involved in the collection of ocean reflections with a GPS receiver. In order to understand quantitatively the sea scattering signature we investigated some of the fundamental features of scattering from ocean surfaces, with particular reference to the effect of wind speed on the surface statistics and scattering cross section. The receiver antenna can then be designed in order to meet power level requirements, whereas the transmitter features are fixed. Our efforts are summarized below.

#### **5.1.1 Footprint determination**

Each GPS satellite transmits two carrier frequencies at L-band ( $L1 \approx 1.6$  GHz, and  $L2 \approx 1.2$  GHz) modulated by a pseudo-random code (P-code), at the rate of 10.23 MHz (30 m wavelength). GPS reflection relies on detecting the amount of energy return of the GPS signal by correlating the pseudo-random code of the transmitted signal and a delayed model of the same code generated in the receiver. At any time the locus of points of equal delay, assuming a reflection is taking place, is a spheroid with the transmitter and the receiver as its foci and focal axis also being the axis of revolution of the generating ellipse. An iso-range contour is defined by the intersection of the ocean surface with a spheroid. The  $n$ -th contour corresponds to points on the surface where delay (distance from transmitter to reflection point to receiver) is  $n$  lags (1 lag =  $1/2$  P-code chip) longer than that of the specular point; it has an approximate elliptical shape. Additionally, a Doppler shift is introduced between the frequency of the transmitted and received signal because of the motion of transmitter and receiver. An iso-Doppler contour is defined by the intersection of the ocean surface and a cone with its vertex at the receiver, its axis along the receiver velocity and the angle corresponding to a given Doppler shift. By examining the power return at different delays, different parts of the ocean are sensed. The footprint of GPS reflection is determined by the intersection of iso-Doppler and iso-range contours as illustrated in Fig. 5.1.

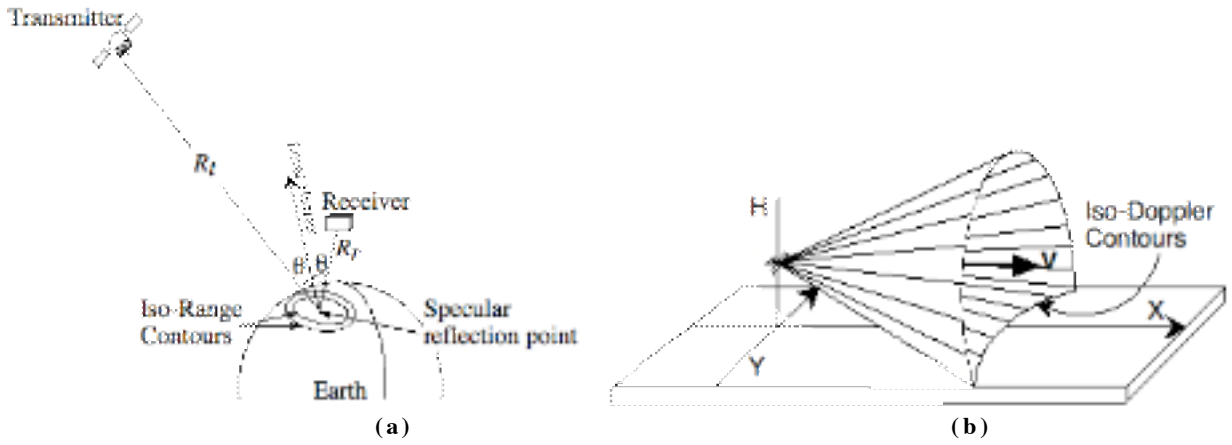


Figure 5.1: (a) Depiction of the bistatic reflection geometry of GPS signal off the Earth surface and the first two iso-range contours. An iso-range contour is defined by the intersection of the ocean surface with a spheroid that has the transmitter and the receiver as its foci. The  $n$ -th contour corresponds to points on the surface where delay (distance from transmitter to reflection point to receiver) is  $n$  lags (1 lag =  $1/2$  P-code chip) longer than that of the specular point; it has an approximate elliptical shape. (b) Iso-Doppler contour is defined by the intersection of the ocean surface and a cone with its vertex at the receiver, its axis along the receiver velocity and the angle corresponding to a given Doppler shift.

Knowing the position of the transmitter and the receiver, the point of specular reflection for a spherical earth is determined geometrically by solving the spherical mirror equation [ Martin-Neira, 1993]. Iso-range ellipses can be determined analytically by intersecting the tangent plane to the spherical earth at the reflection point and the equal-delay spheroids.

As mentioned above, a Doppler shift is introduced in the frequency of the received signal compared to the transmitted one, due to their motion with velocity  $\mathbf{v}_r$  and  $\mathbf{v}_t$ , respectively. Such shift, or bandwidth, is approximated as

$$\Delta f = \frac{1}{\lambda} [\mathbf{v}_t \cdot \mathbf{u}_t - \mathbf{v}_r \cdot \mathbf{u}_r - (\mathbf{v}_t - \mathbf{v}_r) \cdot \mathbf{u}_{rt}] \quad (2)$$

where the unit vector  $\mathbf{u}_t$  is in the direction oriented from the transmitter to the scattering point P on the ocean, the unit vector  $\mathbf{u}_r$  is in the direction oriented from the receiver to the scattering point P, and the unit vector  $\mathbf{u}_{rt}$  is in the direction between the transmitter and the receiver. By observing that the velocity of the transmitter is smaller than that of the receiver, the contribution to Eq. (2) from the first term is ignored while the contribution from the third term amounts to a given fixed offset, which is irrelevant to the calculations. The problem amounts to determining the Doppler footprint on the tangent plane of the ocean surface, corresponding to a given bandwidth. The intersection of such footprint with the range footprint determines the area of ocean which is probed in a single measurement taken with coherent integration time equal to the reciprocal of the Doppler bandwidth. First, the Doppler shift corresponding to the specular point return is obtained, by simplifying (2)

$$\Delta f_0 = v_x \sin(\theta) / \lambda \quad (3)$$

where  $\theta$  indicates the angle of specular reflection about the axis Z. When tracking a GPS reflected signal from a LEO height, phase coherence is expected to be lost in a few milliseconds due to ocean roughness. This, in addition to the generally small reflected signal-to-noise ratio (SNR), makes it unlikely to be able to lock on to the phase, except when the surface is very smooth. However, measurements of pseudorange are possible by coherently correlating the received signal and a delayed version of the P-code over a short time interval (a few msec) and then incoherently averaging the amplitude of thousands of correlation functions obtained over a few seconds. The smallest expected delay,  $L_s$ , roughly corresponds to that of the specular reflection point (determined

to first order from knowledge of the transmitter and receiver positions and the geoid, and then iteratively redefined based on the GPS measurements). The smallest sampled area on the ocean surface is set by the locus of points on the ocean corresponding to delay equal to  $L_s + \Delta$ , where  $\Delta = 1 \text{ lag} \equiv 1/2 \text{ P-code chip}$  and it has the shape of an ellipse. The  $n$ -th annulus is the area between the two ellipses corresponding to delays of  $L_s + (n - 1) \Delta$  and  $L_s + n \Delta$ .

## 5.2 Numerical Results

This section illustrates the results obtained from simulations describing a variety of situations for the most significant parameters of this problem. One important objective of the study is the  $SNR_v$  prediction for realistic sea states, as described by wind speed, and its sensitivity to it. Ultimately, we want to feed the results of this study to the hardware design team, by providing design requirements ranging from the necessary correlator channels to the antenna gain and pointing direction. Naturally, the requirements depend on the kinds of sea state parameters we are interested in extracting, that is to say, mean sea height, wind speed, etc.

The quantity we illustrate as an example is for the case of a receiver located at 700 Km above the Earth, and incident direction of  $38^\circ$  with respect to the Z axis ( $45^\circ$  is the transmitter angle on the horizon of the receiver). The velocity of the receiver is 7 Km/sec along the X direction. Incidentally, this is also the assumed direction for the wind in the calculation of the scattering cross section. In this case we simplify the equation by assuming both the receiver gain and the Doppler modulating function to be unity (in other words, the receiver bandwidth is assumed to be infinite), for the purpose of concentrating on the rise time of the signal and its dependence on wind speed. These features are presented in Fig. 5.2 for four different values of wind speed ( $U_{10}$ ).

We note the following important features of this function: (1) a sharp rise time of  $\sim 1.5$  P-code chips; (2) the sharp rise starts at model delay  $\Delta_n = \Delta_1 - 1$  P-code;

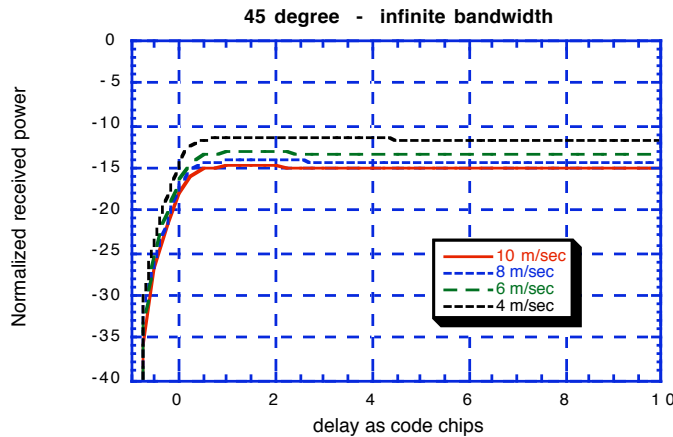


Fig. 5.2 Normalized  $\Delta^2$  versus  $\Delta$  integrated over the footprint assuming infinite receiver bandwidth. The curves are for different wind speed values. The receiver velocity is in the X direction, also taken to be the wind direction.

wind speed, increasing with decreasing value of  $U_{10}$ . By fitting a line to the rising part of this function, the range is estimated to be at 1 P-code chip after the intercept with the abscissa axis; this last kind of measurement is crucial if our instrument is used as an altimeter, whereas the peak value of the curve is significant for its use as a scatterometer.

Note that the rise time is to this accuracy independent of sea state. In reality this will cause the rise time to increase over the value derived here for the ideal correlator function and this information can be used to derive significant wave height.

## 6. Conclusions and future directions

In this task we examined the following issues:

(1) determining the optimal pointing direction and gain of the receiver antenna for a spaced based altimeter sensing GPS signals scattered off the ocean surface. Since the ultimate accuracy is achieved by spatial-temporal averaging of many single shot measurements, each affected by noise, it is stressed that to maximize the sky coverage, and hence the number of available reflections, the receiving antenna must be oriented away from spacecraft nadir. Our investigation shows that away from nadir the coherence integration time is also increased so that a given SNR level can be detected with a smaller receiver antenna gain.

(2) modeling the expected received signal as a function of all the instrument parameters such as geometric configurations, antenna radiation pattern, gain and polarization, correlator channels and receiver bandwidth. Additionally, sea wind speed effects on the scattering properties of the ocean have been quantified. A computer code has been developed and tested which constitutes the preliminary tool for design requirements evaluation as well as an aid in supporting the analysis of acquired data.

We have identified the following items as the logical next steps:

(1) understand sea scattering at low elevation for bistatic configurations to corroborate the preliminary recommendation concerning optimal antenna pointing and gain. This is an area which necessitates some basic EM research, due to the fact that no bistatic instruments have been available to collect data and validate theoretical/numerical models.

(2) continue theoretical work in modeling received signal by describing the effect of sea state on the correlator function, which has been assumed to be ideal in our study. This will allow us to understand the role of significant wave heights on our received signal.

(3) support analysis of data collected with aircraft campaigns.

(4) perform error propagation analysis to understand how the signal to noise ratio maps into the errors in geophysical parameters of interest, such as range, wind and significant wave height.

## 7. References

- Bertiger, W. I., Y. E. Bar-Sever, E. J. Christensen, E. S. Davis, J. R. Guinn, B. J. Haines, R. W. Ibanez-Meier, J. R. Jee, S. M. Lichten, W. G. Melbourne, R. J. Muellerschoen, T. N. Munson, Y. Vigue, S. C. Wu, and T. P. Yunck, B. E. Schutz, P. A. M. Abusali, H. J. Rim, M. M. Watkins, and P. Willis, "GPS Precise Tracking Of Topex/Poseidon: Results and Implications," *JGR Oceans Topex/Poseidon Special Issue*, Vol. 99, 1994, pp. 24449-24464.
- Kursinski, E. R., G. A. Hajj, *et al.*, Initial results of radio occultation observations of Earth's atmosphere using the Global Positioning System, *Science*, 271, 1107-1110, 1996.
- Kursinski E. R. and G. A. Hajj, An examination of water vapor derived from global positioning system occultation observations during June-July 1995, Part I: Zonal Means, submitted to *J. Geophys. Res.*, 1998
- Leroy, S., Measurement of geopotential heights by GPS radio occultation, *J. Geophys. Res.*, 102, 6971-6986, 1997.
- Ware, R., *et al.*, GPS sounding of the atmosphere from low Earth orbit - preliminary results, *Bull. Am. Meteorol. Soc.*, 77, 19-40, 1996.
- Chao, Yi, A. Gangopadhyay, F. O. Bryan, W. R. Holland, 1996, Modeling the Gulf Stream system: how far from reality?, *Geophys. Res. Letts.*, 23, 3155-3158.
- Fu, L-L., and R. D. Smith, 1996, Global ocean circulation from satellite altimetry and high-resolution computer simulation. *Bull. Amer. Meteorolog. Soc.*, 77, 2625-2636.
- Lowe S., 1998, GPS surface reflections SNR estimation, *JPL Interoffice Memorandum*, 335.1-98-009.

Zuffada, C., G. Kaji and E. R. Kursinski, 1998, A novel approach to atmospheric profiling with a down-looking mountain-based or air-borne GPS receiver, submitted to *J. Geophys. Res.*  
Martin-Neira, M., 1993, A Passive Reflectometry and Interferometry System (PARIS): Application to Ocean Altimetry, *ESA Journal*, 17(4), 331-355.